Received November 2003
Revised December 2004
Accepted February 2005

Metal matrix composite processing: numerical study of heat transfer between fibers and metal

Arthur Cantarel, Eric Lacoste and Michel Danis
Laboratoire de Génie Mécanique et Matériaux de Bordeaux (LGM²B), I.U.T. Bordeaux 1 – Domaine Universitaire, Talence Cedex, France, and
Eric Arquis
Laboratoire TREFLE ENSAM/ENSCPB/Univ. Bordeaux1 – CNRS, Site ENSCPB, Pessac, France

Abstract

Purpose – To study heat transfer kinetics at the fiber scale in order to describe injection of liquid metal through a fibrous perform initially situated in a preheated mould, which is one of the various methods used in order to produce metal matrix composite materials (MMCs).

Design/methodology/approach – The first part presents a preliminary study in a static case to describe heat transfer kinetics between a fiber and the matrix in the case of a sudden contact of both components initially set up at different temperatures. This model enables to study the influence of the various parameters of the problem on heat transfer kinetics with phase change. In the second part, we present a modeling which takes into account the metal convection within the pores of the preform.

Findings – The numerical results of these two models justify the instantaneous thermal equilibrium assumption classically admitted to describe MMCs manufacturing methods. The results of this dynamic microscopic model are compared with the results issued from a single temperature macroscopic model to justify the methodological approach and the choice of the microscopic domain geometry representative of the MMCs manufacturing process.

Research limitations/implications – This first numerical model at the microscopic scale deals with the study of heat transfer between fibers and a pure metal. Next step will be the extension of this study to the preform infiltration by a metal alloy. Injection of matrix alloy implies the appearance of phenomena generated by segregation during phase changes.

Originality/value – The results of simulation tests, making use of the usual conditions of MMCs processing, show pretty good agreement with those of macroscopic models describing the anisothermal flow of a pure metal through a porous medium. From this coherence and from the results of the microscopic models as well, the hypothesis of instantaneous thermal equilibrium between fibers and metal (widely used in the literature to study the production of MMCs by infiltration of the liquid metal through the fibrous reinforcement) is justified. Moreover, it will be possible to extend it to the study of infiltration by an alloy, taking then into account thermal and solutal coupled transfers inside the study domain defined in the present work.

Keywords Metals, Heat transfer, Liquid flow, Numerical analysis

Paper type Research paper

International Journal of Numerical Methods for Heat & Fluid Flow
Vol. 15 No. 8, 2005
pp. 808-826

0961-5539
DOI 10.1108/09615530510625093

Introduction

Injection of liquid metal through a fibrous perform initially situated in a preheated mould is one of the various methods used in order to produce metal matrix composite materials (MMCs). In order to reduce the chemical reactions between the fibers and the

metal matrix, the fibrous reinforcement and the mould are generally brought to initial temperatures lower than the solidification temperature of the metal.

These experimental conditions involve local solidification phenomena from the very beginning of injection. In order to avoid costly foundry experiments, theoretical and numerical models, which take into account the strong coupling between mass and heat transfer phenomena, have been performed and applied to the case of infiltration by a single pure metal. In these macroscopic numerical models, the metal saturated preform is assumed to be a continuous medium, and numerical modeling is based on simultaneous and consistent resolutions of Darcy law and continuity equations, with attention to phase change phenomena (Mortensen *et al.*, 1989; Lacoste *et al.*, 1993).

In actual industrial applications, metal alloys are classically used instead of pure metal, then the modelization of the injection is more complex, due to the alloy segregation phenomena: for such alloy injection modelization, it may be tried to simulate the liquid alloy flow at the fiber scale, and then to impose a spatial scale change to describe the process at macroscopic scale.

Our present study deals with pure metal injection at the fiber scale: the objectives of this model are to verify the hypothesis about characteristic thermal equilibrium time, and to test the methodological approach which starts from study at the fiber scale and extends at the macroscopic scale.

This work has been divided into two parts. The first part presents a preliminary study in a static case where convection phenomena resulting from the metal flow around the fibers are not taken into account. Similar modeling has already been developed with the aim to study the evolution of the solidification front: the studied domains are made up of one fiber (Khan and Rohatgi, 1994) or several fibers (Guslick *et al.*, 1999; Arquis and Caltagirone, 1998) surrounded with metal. In these models the two components (matrix and fiber) were initially set up at the same temperature. In our study, the aim is to describe heat transfer kinetics between a fiber and the matrix in the case of a sudden contact of both components initially set up at different temperatures. This model enables to study the influence of the various parameters of the problem on heat transfer kinetics with phase change and the numerical results justify the instantaneous thermal equilibrium assumption classically admitted to describe MMCs manufacturing methods. In second part, we present a modeling which takes into account the metal convection within the pores of the preform. The results of this dynamic microscopic model are then compared with the results issued from a single temperature macroscopic model in order to confirm the instantaneous thermal equilibrium assumption and to justify the methodological approach and the choice of the microscopic domain geometry representative of the MMCs manufacturing process.

Static study

Geometry, initial and boundary conditions

The considered geometry in order to schematize the composite is a one-dimensional parallel periodical network alternately constituted of strata representing, respectively, the fiber and the metal (Figure 1). The stratum depth is related to the porosity of the corresponding fibrous reinforcement. By symmetry, the studied domain (Figure 2) in this model is actually constituted of two parts, one representing "the fiber" (length l_1) and the other "the metal" (length l_2). Length l_1 equals to the 1/2 depth of the reinforcement (i.e. 1/2 diameter of the fiber) and length l_2 is defined from l_1 and from

the porosity of the fibrous preform. Symmetries are expressed by nil flux conditions on the domain boundaries. At the initial instant, the fiber and the pure metal have different temperatures amounting to T_{0p} and T_{0m}, respectively (typically $T_{0p} < T_{sol}$ and $T_{0m} > T_{sol}$).

Dimensionless formulation

The dimensionless formulation of the problem has been achieved from the following reference parameters:

- length l_1;
- thermodynamic characteristics of the fibers: c_f (specific heat) and a_f (thermal diffusivity);
- temperature difference ($T_{sol} - T_{0f}$) between the solidification temperature of the metal (T_{sol}) and the initial temperature of the fiber (T_{0f}); and
- latent heat of the metal (L).

Dimensionless characteristics (mentioned by a prime) of the problem are the following ones:

$$x' = x/l_1;\ t' = \left(a_l/l_1^2\right)t;\ a' = a_i/a_f;\ T' = (T - T_{0f})/(T_{sol} - T_{0f});\ \mathrm{Ste} = c_l(T_{sol} - T_{0f})/L$$

where *Ste* is the Stefan number, characteristic of the phase change phenomenon and i the phase index of the liquid metal ($i = l$), the solid metal ($i = s$) or the fiber ($i = f$).

Numerical results

The numerical model is based upon the discretisation of energy equation (1) with the very classical finite volume method (Patankar, 1980).

$$\frac{\partial T'}{\partial t'} = \nabla \cdot (a^{*\prime} \nabla T') + Q' \tag{1}$$

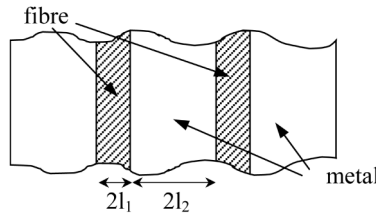

Figure 1.
Modelization of the composite

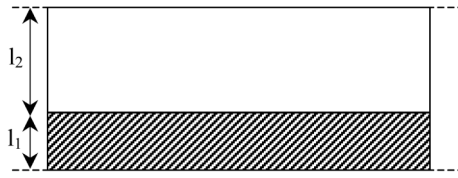

Figure 2.
Studied domain

$a^{*\prime}$ is the thermal diffusivity of the equivalent medium and Q' is a source term which includes the enthalpy release due to phase change.

The method is based on a fixed grid of the studied domain and the source term is calculated using an iterative method (Voller and Prakash, 1987; Voller and Swaminathan, 1991; Mantaux *et al.*, 1995).

As a first step, the equilibrium time τ, that is to say duration to bring the whole domain (fiber and metal) to thermal equilibrium, is calculated as a function of the initial temperature of the metal for peculiar given values. Then, from this reference case, we study the influence of the different parameters (thermodynamic characteristics of the constituents, Stefan number, porosity) on the equilibrium time.

The energy balance is assumed to be reached when dimensional temperature difference ΔT between the hottest and the coldest points of the domain becomes less than $\varepsilon = 10^{-2}$K. If it is obvious that the duration for thermal equilibrium increases as ε decreases, our tests showed that the feature of all the results we are going to present here is not affected by this ε arbitrary choice.

Reference case. After the classical tests of convergence (Figure 3) in order to validate the model, numerical tests have been achieved with the following parameters:

$$a'_s = a'_l = a'_f = 1; \quad \phi = 0.8 \text{ and } Ste = 13.8$$

Moreover, all the simulations of the section are obtained with a dimensionless time step and a dimensionless space step, respectively, fixed at $\Delta t' = 10^{-7}$; $\Delta x' = 0.25$.

By considering the initial dimensionless metal temperature T'_{0m} as varying from 1 to 1.4 per 0.00125 step, we simulated the corresponding heat evolution of the system. Figure 4 summarizes the obtained results in terms of equilibrium time and ultimate solid metal fraction. As a matter of fact, the solid metal fraction is related to a simple calorimetrical assessment, and so, a monotonic duration variation could be expected; however, this variation is far more complex and leads us to distinguish six parts, numbered from 1 to 6 from the lowest initial metal temperatures T'_{0m}. A, B, C, D and E symbolize the boundaries between the different parts. The duration curve for equilibrium exhibits two peaks which are called "peak n°1" for point B and "peak n°2" for point D.

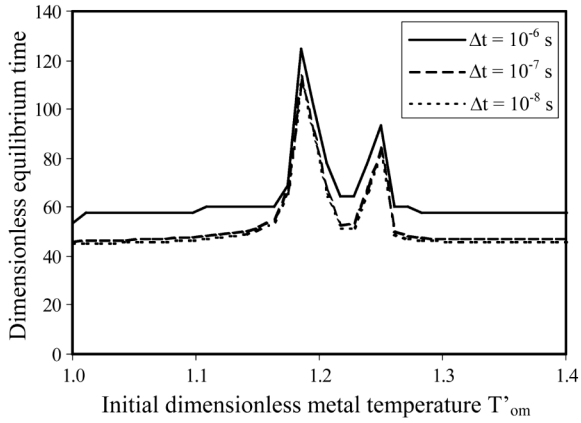

Figure 3.
Test of convergence: influence of the time step $\Delta t'$

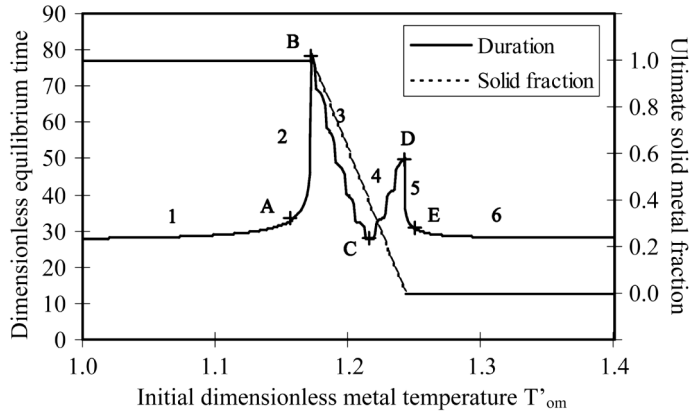

Figure 4.
Duration variation for thermal equilibrium and solid metal fraction vs metal initial temperature for the reference case

Highlighting the influence of phase change. A thorough study of heat transfer kinetics is necessary to explain these results. Figure 5 shows the evolution of the solid metal fraction up to the equilibrium time for points located in the six parts described on Figure 4.

In part 1 (where T_{0m} is near T_{sol}), thermal equilibrium time stead low. We notice that the final solidification fraction always equals to 1, which means that, at equilibrium, metal is completely solidified. Heat transfer kinetics shows that as soon as contact is established between fibers and metal (at the end of a dimensionless time near 10) the whole metal solidifies.

From point A (beginning of part 2), thermal equilibrium time increase. In this part, the phase change from liquid to solid state is slower. This phenomenon increases with T'_{0m}.

From point B (beginning of part 3), the ultimate solid metal fraction is no longer equal to 1; when equilibrium is reached, the metal is thus only partly solidified. When T'_{0m} increases the ultimate solid metal fraction is less and less important and equilibrium time is lower and lower.

From point C (beginning of part 4), heat transfer kinetics shows that in the first time, like in the previous part, a part of the metal is solidified when in contact with the fiber;

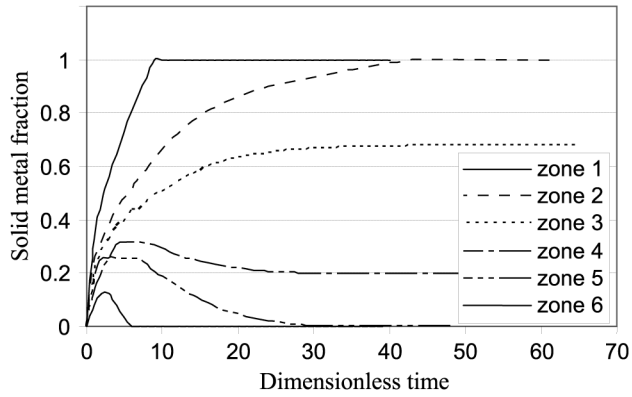

Figure 5.
Evolution of the solid metal fraction in the domain until equilibrium

afterwards a part of the solidified metal is then re-liquefied (metal melting), a phenomenon which does not occur in the two previous parts. This melting phenomenon is all the more important since T'_{0m} increases.

From point D (beginning of part 5), the metal part which has been solidified in the first instants has completely disappeared at equilibrium: the metal is ultimately in a liquid state. The more T'_{0m} increases, the lower is the quantity of solidified metal.

In the last part (part 6), phase change phenomena have almost disappeared and, therefore, have no longer any influence on equilibrium time. This time does not evolve any more and its value is the same as the one obtained for points in part 1.

It is worthy of note that the "wavy shape" of the equilibrium time curve between points B and D is nothing but a typical numerical phenomenon due to the finite volume method used to treat phase change problem (Bell and Wood, 1983).

The complexity of the duration evolution for equilibrium according to the initial metal temperature has led us to study separately the influence of different parameters such as Stefan number, liquid and solid diffusivity or porosity.

Influence of Stefan number. Compared to the results issued from the reference case study ($Ste = 13.8$), influence of Stefan number (with variations of the heat of solidification of the metal L) on duration for thermal equilibrium according to the initial liquid metal temperature for a constant temperature difference $T_{sol} - T_{0f}$ has been investigated (Figure 6). Stefan number increases when energy release during phase change decreases, leading to a reduction of the T'_{0m} interval on which the ultimate solid metal fraction stands partial. On Figure 6, this result is expressed by narrowing the first and second peak interval as *Ste* increases, point D keeping almost the same location. Evolution of duration for thermal equilibrium of the domain according to T'_{0m} is very slightly disturbed by the variations of Stefan number. A displacement of the different parts of the curve is only observed.

Influence of metal's thermal diffusivity. Influence of solid metal's thermal diffusivity a'_s, by keeping constant parameter a'_1 is now estimated (Figure 7(a)). The equilibrium time strongly decreases in the first half of the domain (which corresponds to the first three parts shown in Figure 4) when a'_s increases. This decrease of thermal equilibrium time results from the increasing diffusivity (generated by increasing of the thermal conductivity) in the solid metal, which is the prevailing phase of the first part of the

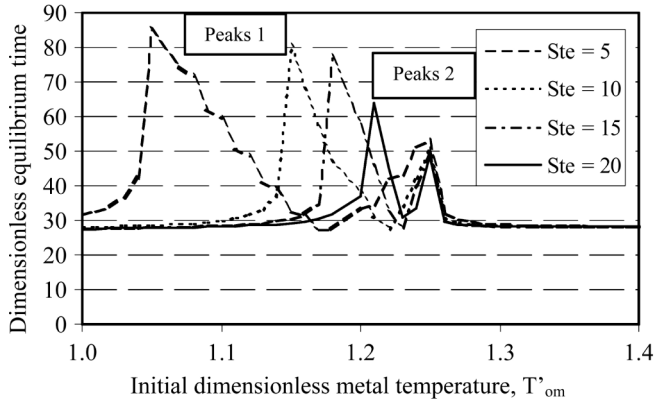

Figure 6.
Influence of Stefan number on the duration variation for thermal equilibrium vs initial temperature of the liquid metal

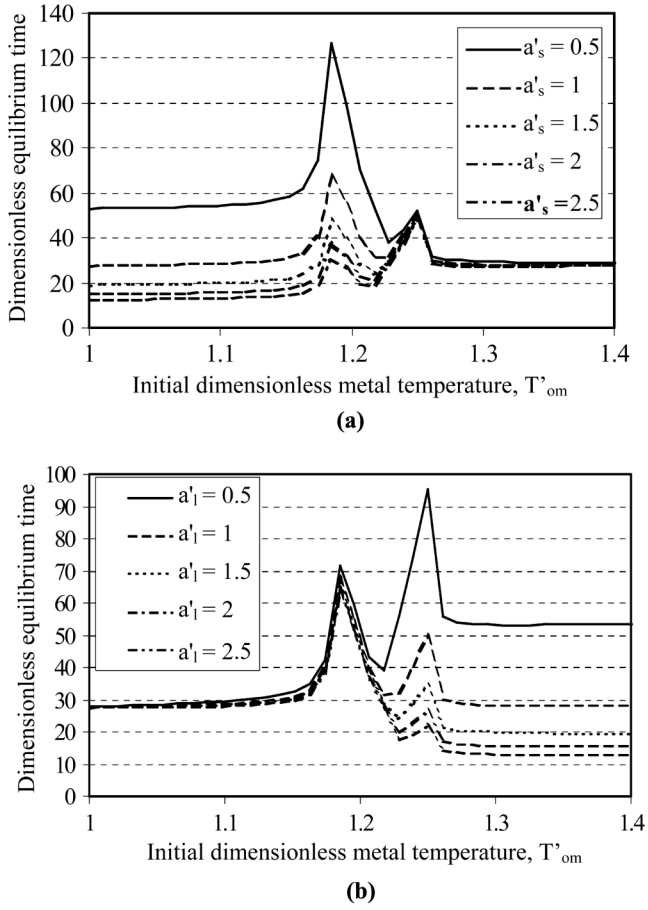

Figure 7.
Influence of the metal thermal diffusivity on the duration variation for thermal equilibrium vs initial temperature of the liquid metal; (a) thermal diffusivity of the solid metal; and (b) thermal diffusivity of the liquid metal

curve ($T'_{0m} < 1.22$). In the second part ($T'_{0m} > 1.22$), as solid fraction is low, the influence of a'_s decreases.

Similarly, by making a'_l diffusivity of the liquid metal vary and by keeping parameter a'_s constant, thermal equilibrium time of the domain strongly decreases in the second half of the domain, which corresponds to the last three parts shown in Figure 4 (initial metal temperatures T'_{0m} more than 1.22) when a'_l increases (Figure 7(b)). Indeed, the liquid phase prevails in the second part of the curve and consequently this phenomenon has a preponderant influence in this part.

Influence of porosity. Porosity is the last parameter chosen for this study (Figure 8). The reference length chosen as dimensionless parameter is the one characteristic of the fiber, that is to say l'_1 which has been set to *1*. Therefore, a decreasing porosity is significant of a more compactness of the fibrous preform. Increasing porosity generates increasing of the metal's quantity (l'_2), which is correlated on the curves by an increase of equilibrium time. Furthermore, when l'_2 increases, the quantity of heat brought by the metal matrix increases while energy due to the fibers remains constant. The initial

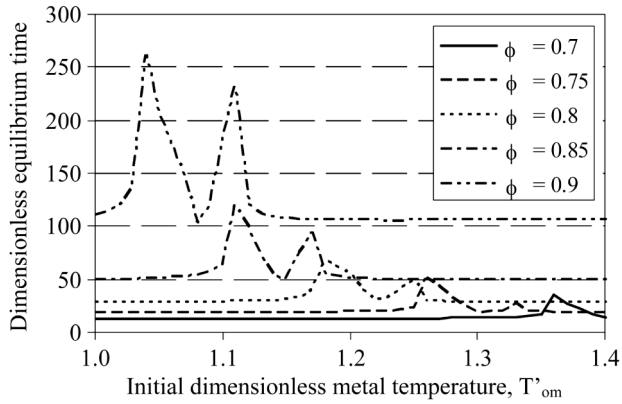

Figure 8.
Influence of porosity on the duration variation for thermal equilibrium vs initial temperature of the liquid metal

temperature T'_{0m}, for which the final solidification fraction remains equal to 1, is then lower and lower, which explains the earlier and earlier appearance of the first peak associated to the increase in porosity.

Presence of equilibrium times peaks. The presence of such peaks may be explained by the phase change which occurs at an imposed and constant temperature (pure metal). As a matter of fact, the domain point where the phase change does occur is the phase change temperature $T'_{sol} = 1$, and conductive transfer is proportional to the temperature gradient. The higher is this gradient, the more important is the flux energy and the faster is the heat transfer. Any volume implied in a phase change absorbs an important quantity of energy L and consequently slows down heat exchanges between solid and liquid parts. These exchanges are all the slower since the temperature gradient is low between the solid/liquid interface and the other parts of the domain. This slackening effect is emphasized twice:

(1) first when the maximum temperature T'_{0m}, for which the matrix is both entirely solid and isothermal (peak $n°1$), is reached; and

(2) second when the minimum temperature T'_{0m}, for which the matrix is both entirely liquid and isothermal (peak $n°2$), is reached.

Practical illustration. This first study enables us to understand heat transfer kinetics when fibers and matrix are brought into contact in a static case, and to calculate the duration for thermal equilibrium of both components. Previous studies about processing of MMCs by metal injection through fibers have shown the existence of a front zone, from the beginning of impregnation onwards, where metal is at its solidification temperature T_{sol} (Lacoste *et al.*, 1993). Inside that zone, fibers at an initial temperature T_{0f} are impregnated by a metal at temperature T_{sol}. For a fibrous perform, constituted of graphite fibers with a porosity of 0.8, initially preheated to 200°C and impregnated by pure aluminium, the computed thermal equilibrium time making use of the static model is about 10^{-5} s. So, for a flowing metal's speed through the preform taken as 10^{-1} m.s^{-1}, the thermal equilibrium domain is less than one micron large. Thus, the instantaneous equilibrium assumption, classically used in the single temperature models applied to liquid-state MMC processing, seems to be justified. However, the assumption of a static model somehow restricts its application.

The aim is now to define a representative microscopic study domain and to take into account convection phenomena generated by the metal's flow through the fibrous network when processing MMCs by injection methods. This dynamic model also justifies the choice of a representative domain geometry to study manufacturing process, and some preliminary results of metal alloy injection model were obtained with this microscopic domain geometry (Cantarel, 2004).

Dynamic study

Microscopic model

The considered geometry in order to modelize the fibrous preform is similar to the one described in the previous paragraph. The domain is made up of a periodical stacking up of parallel layers. By symmetry, the domain geometry, which allows the study of the metal flow, reduces to a bi-dimensional pipe bounded by two parallel slabs whose thickness are those of a half stratum (Figure 9). The bi-dimensional problem consists in studying a two-phases flow involving two non-miscible fluids (pure metal and air), coupled with phase change phenomena (metal melting and solidification).

The final purpose is to compare the results of this microscopic dynamic model with those of a macroscopic model previously published in the literature (Mortensen *et al.*, 1989; Lacoste *et al.*, 1993). At the opposite of the previous, and somehow more phenomenological, static study where dimensionless parameters have been used, here, dimensional parameters are used.

Assumption on metal/air interface. The metal flow between the slabs is assumed to be laminar ($Re_c \approx 2$ and $Re < 1$). To describe the metal flow, the interface position at each instant must be known. In a rigorous and complete approach, this study would require to know the surface tensions between the fluids and the fiber wall ($\sigma_{solid/metal}$ et $\sigma_{solid/air}$) and the surface tensions between the liquid metal and air (σ metal/air) which verify Young's equation:

$$\sigma_{solid/air} - \sigma_{solid/metal} = \sigma_{metal/air} \cos \theta \tag{2}$$

where θ represents the contact angle between the liquid metal and the solid reinforcement.

These parameters indeed depend not only on the present fluids, here liquid metal and air, on the nature of the solid (which has been defined from the characteristics of fibers) but also on flow conditions (pressure and temperature). Taking into account these parameters in the models is very tricky and must be studied thoroughly from an experimental as well as from a numerical point of view (Fukai *et al.*, 1995).

The interface modeling also faces difficulties due to the boundary conditions of the problem. If for a one phase flow, velocities are nil at the slab walls, this condition is not verified at the triple point (metal/fiber/air) in the case of a two phase flow because of the interface displacement. A classical method consists in admitting the possibility of

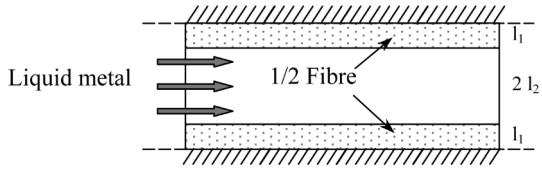

Figure 9.
Studied domain for the dynamic case

the metal sliding on the edge and in giving sliding velocities in the neighborhood of the contact between the interface and the edges (Van Quy, 1971).

Our purpose here is the study of heat exchanges during the flow. If exchanges with air are negligible versus exchanges between the wall and the metal, a strict knowledge of the geometry of the metal front is no more necessary. The assumption that we have chosen is to consider that the metal front remains plane with a displacement velocity equaling the metal's injection velocity. From afar of the metal front, an adherence condition to solid reinforcement has been imposed in both air and liquid. Imposing a sliding to the contact of fibers close to the triple point at the metal/air interface as well as the geometry of the metal front has a very slight influence on heat exchanges, which we verified with various computations (not presented here).

Numerical model. The metal flow is described by the mass balance equation (3) and Navier-Stokes equation in which effects generated by gravity are neglected (equation (4)):

$$\nabla \cdot U = 0 \tag{3}$$

$$\rho\left(\frac{\partial U}{\partial t} + (U \cdot \nabla)U\right) = -\nabla p + \mu \nabla^2 U \tag{4}$$

where U is the velocity and p the pressure; U and ρ are, respectively, the density and the dynamic viscosity of the liquid metal. The metal is considered as a newtonian fluid whose viscosity does not depend on temperature. The solidified metal viscosity is considered as infinite. To solve the flow problem taking into account modifications due to the apparition of solidification, we introduce finely the Brinkman equation (5).

$$\rho\left(\frac{\partial U}{\partial t} + (U \cdot \nabla)U\right) = -\nabla p + \mu \nabla^2 U - \frac{\mu}{K} U \tag{5}$$

$(\mu/K)U$ being a penalization term which allows to define the nature of the medium: if the terms of K are equal to zero, metal is liquid and if the terms of K tend to infinity, metal is solid. The coupling equations (3) and (5) are solved with a hybrid method where the projection method (Goda, 1978) is coupled with an augmented Lagrangian method (Fortin and Glovinski, 1982). Indeed, the augmented Lagrangian and the projection method are less efficient because of the strong density and viscosity gradients near the interface. The algorithm of this hybrid augmented Lagrangian-Projection method is detailed in Vincent and Caltagirone (1999).

The heat equation (6) with phase change phenomena is solved from a source term model (Mantaux *et al.*, 1995) and a T.V.D. scheme for the convective term (Sweby, 1984). The complete formulation of the numerical method used for the heat transfer problem is described by Del Borrello and Lacoste (2003).

$$\rho C\left(\frac{\partial T}{\partial t} + U \cdot \nabla T\right) = \nabla \cdot (\lambda \nabla T) + Q \tag{6}$$

λ is the tensor of thermal conductivity of the medium (ρc) is the volumetric heat capacity of the medium and Q is a source term which includes the enthalpy release due to phase change.

The thermal contact resistances between the fibers and the metal matrix as well as radiation are neglected. The flow and the heat transfer problems are then coupled, which modelizes phase change phenomena during MMCs processing.

Initial and boundary conditions. In addition to the assumptions on the metal/air interface (paragraph 3.1.1), the other initial and boundary conditions of the problem are the following ones:

- the metal is injected parallel to strata at a constant velocity V_0 and at T_{0m} temperature, constant in time and greater than the phase change temperature of the metal T_{sol};
- fibers are initially at a T_{0f} temperature; and
- because of the studied geometry the problem comes down to the study of a metal flow between two slabs whose thickness is the thickness of a "half fiber". Owing to symmetry conditions, the upper and lower boundaries of the domain are adiabatic boundaries.

Micro-macro comparison

The aim of this part is to compare the results of macroscopic theoretical models (what we shall shortly recall), to those issued from the present microscopic dynamic model.

Monodimensional macroscopic model. The macroscopic theoretical models are based upon the computation of a continuity equation coupled with Darcy's law and of the energy equation with phase change phenomena (Mortensen *et al.*, 1989; Lacoste *et al.*, 1993). We studied a 1D configuration with adiabatic mould walls for which analytical solutions exist. This is a single temperature model. Assuming the metal saturated preform to be an homogeneous medium whose equivalent thermal conductivity λ^* and equivalent specific heat $(\rho C)^*$ are given by relations (7) and (8):

$$\lambda^* = \lambda_m \cdot \phi + \lambda_f \cdot (1 - \phi) \tag{7}$$

$$(\rho C)^* = (\rho C)_m \cdot \phi + (\rho C)_f \cdot (1 - \phi) \tag{8}$$

where λ_m and λ_f are the thermal conductivities of the metal and of the fibers respectively; $(\rho C)_m$ and $(\rho C)_f$ are the specific heats of the metal and the fibers, respectively, and ϕ is the porosity of the fibrous preform. Parameters λ_m and $(\rho C)_m$ are calculated from relations similar to relations (7) and (8) with the liquid or solid metal parameters, and from the liquid/solid proportion in the considered volume instead of fiber parameters and porosity.

The metal flow through the fibrous preform is described by Darcy in equation (9) and mass balance in equation (10).

$$V = -\frac{K}{\mu}\frac{\partial p}{\partial x} \tag{9}$$

$$\nabla \cdot V = 0 \tag{10}$$

where K is the permeability of the fibrous preform and V Darcy velocity.

Assuming the fibrous preform to be dimensionally stable and the metal to be uncompressible, the metal/air interface position, $X_m(t)$, at an instant t is given as follows:

$$X_{\mathrm{m}}(t) = \frac{V_0 \cdot t}{\phi} \tag{11}$$

where V_0 is the metal injection velocity and ϕ the fibrous preform porosity. If V_0 is high enough, the conduction in the flow direction may be neglected as compared with advection heat exchanges. The heat problem, therefore, comes down to the solving of the following equation:

$$(\rho C)^* \frac{\partial T}{\partial t} = -(\rho C)_l V \frac{\partial T}{\partial x} \tag{12}$$

where $(\rho C)_l$ represents the specific heat of the liquid metal.

Two cases must be studied: the case for an initial fibers temperature $T_{0\mathrm{f}}$ higher than T_{sol} (absence of phase change phenomena) and the case where $T_{0\mathrm{f}}$ is lower than the solidification temperature of the metal T_{sol} (presence of phase change phenomena).

For the case where $T_{0\mathrm{f}} > T_{\mathrm{sol}}$, the metal is not solidified when in contact with fibers. The heat problem makes a thermal front to appear, which is delayed compared with the metal front (Figure 10). Its position X_{T} is given by (13).

$$X_T = \frac{\phi(\rho C)_l}{(\rho C)^*} X_{\mathrm{m}} \tag{13}$$

For the case where $T_{0\mathrm{f}} < T_{\mathrm{sol}}$, there are phase change phenomena. The heat problem makes two heat fronts to appear, which separate three distinct parts whose inside the temperatures are constant (Figure 11):

(1) part 1: downstream the metal front where the preform has not been impregnated yet; the temperature remains to the initial temperature $T_{0\mathrm{f}}$;

(2) part 2: constituted by the preform impregnated by a partly solidified metal; in this part the temperature reaches to the phase change temperature T_{sol} and simultaneously the solid metal fraction Fs is constant; and

(3) part 3: where the preform has been impregnated by the entirely liquid metal; the temperature arises to $T_{0\mathrm{m}}$, the injection temperature.

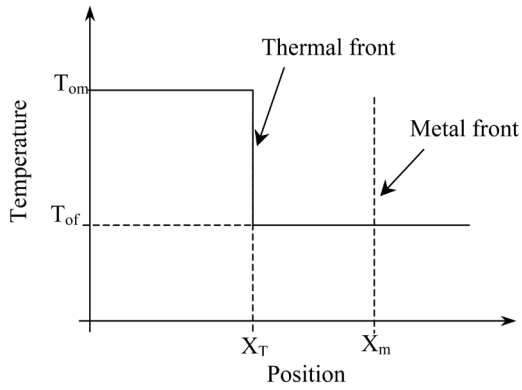

Figure 10.
Impregnation of a fibrous preform by a liquid metal for an adiabatic case when the initial temperature of fibers is higher than the metal solidification temperature

Considering a simple calorimetric balance allows to calculate the F_S proportion of solidified metal in part 2 (equation (14)) as well as the X_T position of the thermal front (equation (15)).

$$F_S = \frac{(1-\phi)(\rho C)_f (T_{sol} - T_{0f})}{\phi L_S} \tag{14}$$

$$X_T = \frac{(\rho C)_l \phi}{(\rho C)^* + (1-\phi)(\rho C)_l \left(\frac{T_{sol} - T_{0f}}{T_{0m} - T_{sol}}\right)} X_m \tag{15}$$

Comparison of 2D microscopic and 1D macroscopic models. In a first step, results of the 2D microscopic dynamic model, with realistic parameters from a point of view of the production process (Table I), are shown.

Preliminary simulation have been performed to test the convergence. Figures 12 and 13 exhibit the influence of the space steps (Δx and Δy) in a case without phase change. Afterwards, for all the other simulations presented in the section, the numerical parameters are the following: $\Delta t = 10^{-5}$ s; $\Delta x = 4.10^{-6}$ m and $\Delta y = 1.10^{-6}$ m.

In order to simulate a case without phase change, we chose a $T_{0f} = 661$°C temperature, higher than T_{sol} ($T_{sol} = 660$°C). The resulting 2D temperature field is shown in Figure 14 and particularly highlights the single directional character of the phenomena: the temperature is uniform along all the domain width. The presence of a heat "plateau" is the same as noticed on the macroscopic model. Figure 15 shows a good accordance between results of the two computation models.

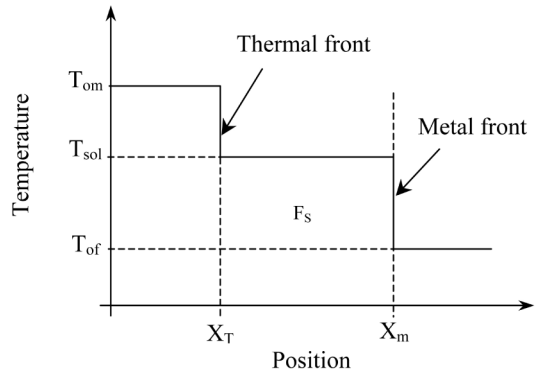

Figure 11.
Impregnation of a fibrous preform by a liquid metal for an adiabatic case when the initial temperature of fibers is lower than the metal solidification temperature

Reinforcement or fiber	Carbon (width 5×10^{-6} m) (Appendix)
Porosity	0.75
Matrix	Pure aluminium (Appendix)
Metal injection velocity	0.04 m.s^{-1}
Metal injection temperature	800°C
Domain length	2×10^{-4} m
Domain width	2×10^{-5} m

Table I.
Parameters example for the MMCs processing

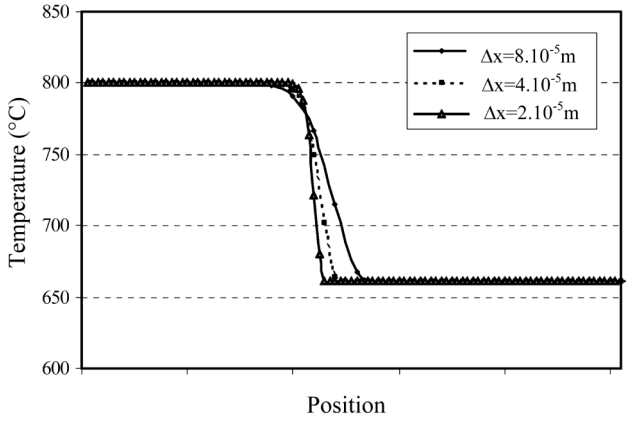

Figure 12.
Test of convergence: influence of the space step Δx

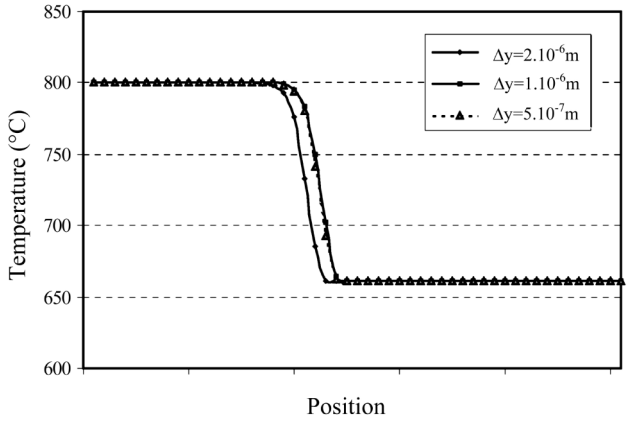

Figure 13.
Test of convergence: influence of the space step Δy

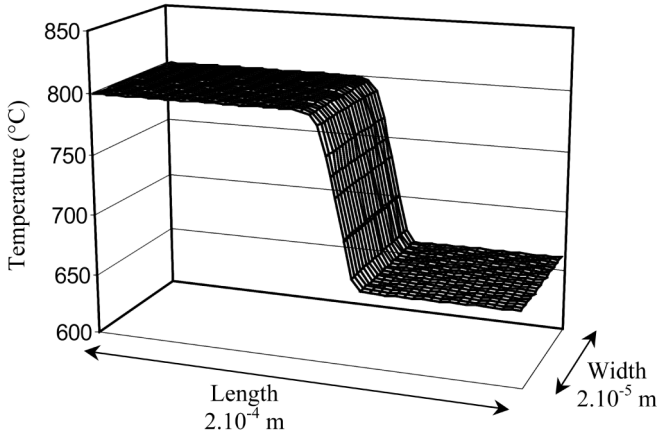

Figure 14.
Numerical results of the 2D microscopic dynamic model without phase change

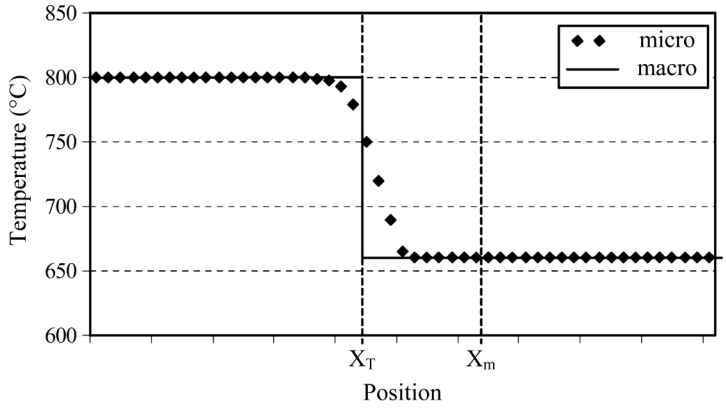

Figure 15.
Comparison between the 2D microscopic and the 1D macroscopic models for a case without phase change

In order to confirm this accordance, the duration of thermal equilibrium between fiber and metal has been estimated by computing the evolution of the maximum temperature difference ΔT obtained in the studied domain width within different sections (Figure 16). For any given section S_i, the curve may be divided into three distinct parts (Figure 16):

(1) a domain where ΔT is equal to zero: the thermal front has not reached S_i yet;

(2) a second domain where ΔT is different to zero; during this time, the thermal front is passing through S_i;

(3) a domain where ΔT is again equal to zero: the thermal front is now farther than S_i.

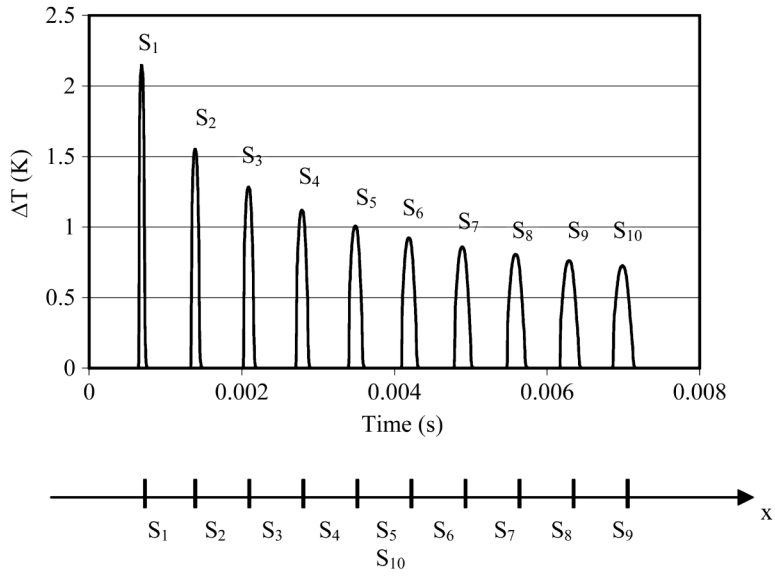

Figure 16.
Evolution of the maximum difference ΔT for different sections of the studied domain

The second domain length is related to the thermal equilibrium time. From the example shown in Figure 16, we may then deduce that the duration for thermal equilibrium is less than 10^{-4}s for any section S_i. These results confirm those obtained from the preliminary static study and then once more justify the instantaneous equilibrium assumption used to simulate manufacturing of MMCs.

In the case where the initial temperature of fibers is less than T_{sol} ($T_{0f} = 300$°C), the temperature field (Figure 17) exhibits two temperature "plateaux" as for the macroscopic model. Besides, the temperature is almost uniform along all the domain width whatever the X-position.

Figure 18 shows a very good agreement between the results of the full 2D microscopic and the 1D macroscopic models as far as the temperature field is concerned, as well as for solidification fractions are concerned.

Influence of the longitudinal conductivity. All the results presented in this paper are based upon the hypothesis that the longitudinal conductivity is negligible. In order to justify the validity of this hypothesis, longitudinal conductivity has been integrated in this microscopic dynamic model. Then, the thermal regime is evaluated thanks to the Peclet number: $Pe = (V_0 l)/a^*$ where l is equal to $2(l_1 + l_2)$ (Figure 2) and a^* is

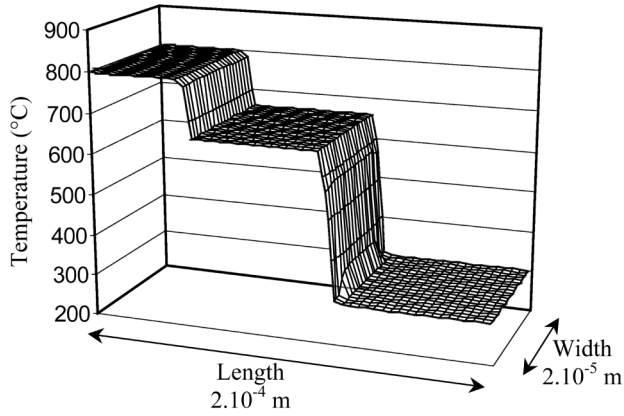

Figure 17.
Numerical results of the 2D microscopic dynamic model for a case with phase change phenomena

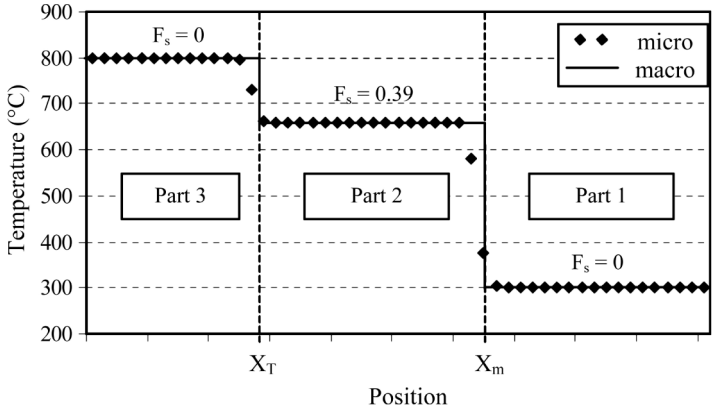

Figure 18.
Comparison between the 2D microscopic and the 1D macroscopic models for a case with phase change phenomena

the diffusivity of the equivalent medium. Numerical results show that the hypothesis is justified when the Peclet number is large enough ($Pe > 1$), which is an usual estimated value for such combined conduction/convection problem. Figure 19 shows the results of the 2D microscopic model taking into account the conduction in the flow direction: it is worthy of note the good agreement between these results and those obtained with the 1D macroscopic model (see precedent section). On the other hand, our numerical tests show that conduction in the flow direction cannot be neglected when the Peclet number is less than 1 (Figure 20): in this case, the heat transfers by conduction are predominant. However, the results show also that the temperature difference between fibers and metal remains very low.

Ultimately, the hypothesis that the thermal conductivity in the flow direction is negligible is justified for the usual conditions of MMCs production ($Pe > 1$). Moreover, this study shows also that the hypothesis of instantaneous thermal equilibrium between fibers and metal, used in the macroscopic models, is justified whatever the Peclet number value may be.

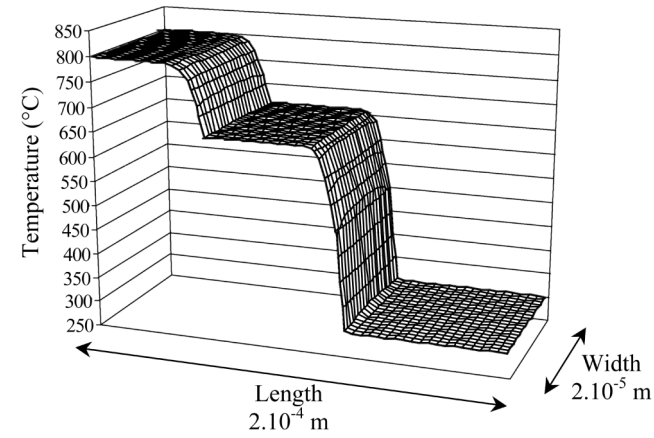

Figure 19.
Numerical results of the 2D microscopic dynamic model with phase change phenomena, taking into account of the thermal conductivity in the flow direction ($Pe = 10$)

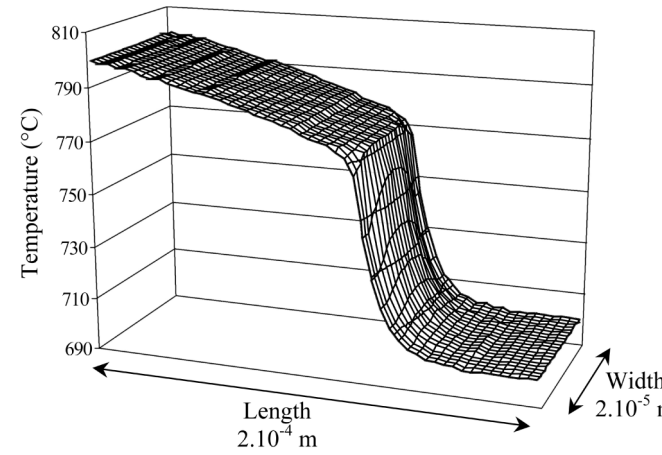

Figure 20.
Numerical results of the 2D microscopic dynamic model without phase change taking into account of the thermal conductivity in the flow direction ($Pe = 0.1$)

Conclusion and perspective

In this work, we develop a numerical modeling of heat transfer between a fibrous reinforcement and a pure metal taking into account phase change phenomena at the fiber scale. A first static model studies the duration for thermal equilibrium when the fibers and the melting metal are in contact. A second dynamic model describes the metal flow in the case of a pure metal between two slabs representing the fibrous reinforcement. This model takes into account phase change phenomena and convection transfers. The results of simulation tests, making use of the usual conditions of MMCs processing, show pretty good agreement with those of macroscopic models describing the anisothermal flow of a pure metal through a porous medium. From this coherence and from the results of the microscopic models as well, the hypothesis of instantaneous thermal equilibrium between fibers and metal (widely used in the literature to study the production of MMCs by infiltration of the liquid metal through the fibrous reinforcement) is justified.

This first numerical model at the microscopic scale deals with the study of heat transfer between fibers and a pure metal. Next step will be the extension of this study to the preform infiltration by a metal alloy. Injection of matrix alloy implies the appearance of phenomena generated by segregation during phase changes. A model has been recently developed for a static configuration (Moussa *et al.*, 2002). It will be possible to extend it to the study of infiltration by an alloy, taking then into account thermal and solutal coupled transfers inside the study domain defined in the present work: first preliminary numerical results were obtained using such domain geometry (Cantarel, 2004).

References

Arquis, E. and Caltagirone, J.P. (1998), "Solidification in heterogeneous media: a numerical study at a small scale", in Thomas, B.G., Beckermann, C. and Oknada, I. (Eds), *Proceedings of the Modeling of Casting, Welding and Advanced Solidification Processes VIII*, pp. 581-8, TMS, Warrendale, PA, San Diego, CA.

Bell, G.E. and Wood, A.S. (1983), "On the performance of the enthalpy method in the region of a singularity", *International Journal for Numerical Methods in Engineering*, Vol. 19, pp. 1583-92.

Cantarel, A. (2004), "Modélisation de l'imprégnation d'une préforme fiberuse par un alliage en vue de l'élaboration de matériaux composites à matrice métallique", PhD thesis, University of Bordeaux 1, Talence Cedex.

Del Borrello, C. and Lacoste, E. (2003), "Numerical simulation of the infiltration of a porous medium by a pure body: application of the elaboration of metal matrix composites", *Numerical Heat and Mass Transfer, Part A*, Vol. 44 No. 7, pp. 723-41.

Fortin, M. and Glovinski, R. (1982), "Méthodes de Lagrangien augmenté", *Application à la résolution numérique de problèmes aux milites*, Dunod, Paris.

Fukai, J., Shiiba, Y., Yamamoto, T., Miyatabe, O., Poulikakos, D., Megaridis, C.M. and Zhao, Z. (1995), "Wetting effects on the spreading of a liquid droplet colliding with a flat surface: experiment and modelling", *Physic Fluids*, Vol. 7, pp. 236-47.

Goda, K. (1978), "A multistep technique with implicit difference schemes for calculating two or three dimensional cavity flows", *Journal of Computational Physics*, Vol. 30, pp. 76-95.

Guslick, M.M., Simpson, J.E. and Garimella, S.V. (1999), "Fiber-spacing effects in the solidification processing of metal matrix composites", *Numerical Heat Transfer Part A*, Vol. 35, pp. 587-607.

Khan, M.A. and Rohatgi, P.K. (1994), "Numerical solution to a moving boundary problem in a composite medium", *Numerical Heat Transfer Part A*, Vol. 25, pp. 209-21.

Lacoste, E., Aboulfatah, M., Danis, M. and Girot, F. (1993), "Numerical simulation of the infiltration of fibrous preform by a pure metal", *Metallurgical Transactions A*, Vol. 24A, pp. 2667-78.

Mantaux, O., Lacoste, E. and Danis, M. (1995), "Conduction avec changement de phase dans un corps pur: résolution en température", *Revue Générale de Thermique*, Vol. 402 No. 34, pp. 339-47.

Mortensen, A., Masur, L.J., Cornie, J.A. and Flemings, M.C. (1989), "Infiltration of fibrous preforms by a pure metal: Part I. Theory", *Metallurgical Transactions A*, Vol. 20A, pp. 2535-46.

Moussa, B., Simpson, J.E. and Garimella, S.V. (2002), "Concentration fields in the solidification processing of metal matrix composites", *International Journal of Heat and Mass Transfer*, Vol. 45, pp. 4251-66.

Patankar, S.V. (1980), *Numerical Heat Transfer and Fluid Flow*, Hemisphere, New York, NY.

Sweby, P.K. (1984), "High resolution schemes using flux limiters for hyperbolic conservation laws", *Siam Journal of Numerical Analysis*, Vol. 21, pp. 995-1011.

Van Quy, N. (1971), "Sur l'écoulement entre deux plaques parallèles voisines, de deux fluides séparés par une interface", *International Journal of Engineering Science*, Vol. 9, pp. 101-32.

Vincent, S. and Caltagirone, J.P. (1999), "Efficient solving method for unsteady incompressible interfacial flow problems", *International Journal for Numerical Methods in Fluids*, Vol. 30, pp. 795-811.

Voller, V.R. and Prakash, C. (1987), "A fixed grid numerical modeling methodology for convection/diffusionmushy region phase change problems", *International Journal Heat and Mass Transfer*, Vol. 30, pp. 1709-19.

Voller, V.R. and Swaminathan, C.R. (1991), "General source-based method for solidification phase change", *Numerical Heat Transfer, Part B*, Vol. 19, pp. 175-89.

Appendix

Aluminium parameters

$\lambda_l = 90\,\mathrm{W\,m^{-1}K^{-1}}$

$(\rho c)_l = 2.5 \times 10^6\,\mathrm{J\,m^{-3}K^{-1}}$

$\lambda_s = 150\,\mathrm{W\,m^{-1}K^{-1}}$

$(\rho c)_s = 2.9 \times 10^6\,\mathrm{J\,m^{-3}K^{-1}}$

$L = 0.93 \times 10^9\,\mathrm{J\,m^{-3}}$

$\mu = 10^{-3}\,\mathrm{Pa.s}$

Carbon fiber parameters

$\lambda_f = 8.9\,\mathrm{W\,m^{-1}K^{-1}}$

$(\rho c)_f = 3 \times 10^6\,\mathrm{J\,m^{-3}K^{-1}}$